

Indentation Analysis of a Multi-Layered Hollow Cylinder for the Measurement of Interfacial Toughness in TBC Systems

Q. Ma^{1,2}, J. L. Beuth¹, G. H. Meier³ and F. S. Pettit³

Summary

This paper addresses the mechanics of indentation-induced delamination of a coating on a multi-layered hollow cylinder, for application to toughness testing of thermal barrier coating (TBC) systems. An electron-beam physical vapor deposition (EB-PVD) TBC system has been analyzed through a contact finite element model using a standard conical indenter impressed vertically on the top of the cylinder. Two cylinder sizes used in thermal-mechanical fatigue tests in literature have been considered in the analysis, with outer radii of 5.11 mm and 3.08 mm, and inner radii of 3.00 mm and 0.97 mm, respectively. Two boundary conditions for the inner surface of each cylinder, traction free and constrained radial displacement, have been considered in the numerical studies. It is shown that stress intensity factor distributions in the axial direction on the cylinder surface are close to corresponding 2-D results for the indent test load levels of interest. Consequently, with regard to the measurement of interfacial toughness, the complex 3-D analysis can be understood using 2-D simulation results. At the same time, 3-D results are also found to be important in identifying valid indentation tests avoiding buckling driven delamination.

Introduction

Existing work by the authors has addressed axisymmetric delamination of thermal barrier coatings (TBCs) deposited onto flat substrates (disc-shaped specimens) [1-6]. The application of interest is indentation fracture toughness testing of TBC systems, where indentation by a conical indenter through the coating and into the substrate induces axisymmetric debonds. Fracture mechanics-based analyses of these tests allow debond sizes to be related to the interfacial fracture toughness. In practice, however, ceramic thermal barrier coatings are deposited onto turbine blades and other components with curved surfaces. A natural question that arises is how toughness can be measured through similar tests on curved specimens.

Recent research at the German Aerospace Center Institute of Materials Research, involving thermal gradient mechanical fatigue (TGMF) tests on EB-PVD

¹Department of Mechanical Engineering, Carnegie Mellon University, Pittsburgh, PA 15213, USA. Now with EFC School of Engineering, Walla Walla University, College Place, WA 99324, USA

²Now with EFC School of Engineering, Walla Walla University, College Place, WA 99324, USA

³Department of Mechanical Engineering & Materials Science, University of Pittsburgh, PA 15261, USA

TBC systems [7] has considered indentation testing on curved substrates. The specimens used in these tests are hollow cylinders with various inner and outer diameters, simulating the exposure of gas turbine blades by imposing simulated mechanical fatigue loads in addition to thermal cycles. Cooling air is circulated in the hollow cylinders to induce a thermal gradient similar to that seen in air-cooled turbine blades.

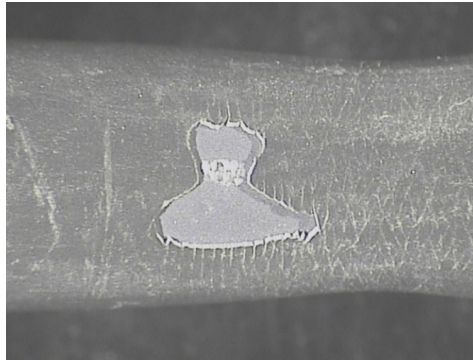


Figure 1: elamination pattern of a TBC coating on a cylindrical specimen with outer diameter = 14.7 mm, inner diameter = 6 mm, NiCoCrAlY bond coat thickness = 110 μm , and EB-PVD TBC thickness = 220 μm [7].

After some TGMF specimens were tested, they were indented at room temperature by a Brale conical indenter to induce debonding. It was observed that the delamination, caused by the combination of biaxial residual stresses in the TGO and TBC layers and the induced stresses due to indentation, can yield a butterfly-shaped debonding pattern, as shown in Fig. 1. Understanding this debonding pattern is important to the development of indentation tests for these specimens. Besides the TGMF tests in Germany, another widely used method for the study of TBC degradation mechanisms is the burner rig test (BRT) [8]. A BRT typically uses cylindrical specimens. To track adhesion loss in BRT TBC systems, development of a method similar to indentation tests on disc-shaped specimens is needed, such that the interfacial fracture toughness can be determined at various fractions of TBC life before spontaneous failure occurs.

The purpose of this study is thus to develop a practical approach for measuring interfacial fracture toughness for TBCs deposited onto curved substrates through detailed numerical analyses for contact on hollow cylinders. A quantitative analysis of surface strain distributions in each direction (longitudinal vs. circumferential) is performed through 3-D finite element simulations. These analyses allow the determination of steady state energy release rates and interfacial toughnesses for this type of test. Furthermore, it is demonstrated that stress intensity factors are strongly

directional dependent with results in the axial direction close to corresponding 2-D flat specimen results.

Geometrical Aspects and Dimensional Analysis for Surface Strains

Figure 2 (a) gives a schematic of the indentation geometry. Because the radius of the cylinder is much larger than the indentation size, to simplify the analysis, we may imagine another indenter operating from its opposite side. Therefore, it is only necessary to simulate one-eighth of the specimen.

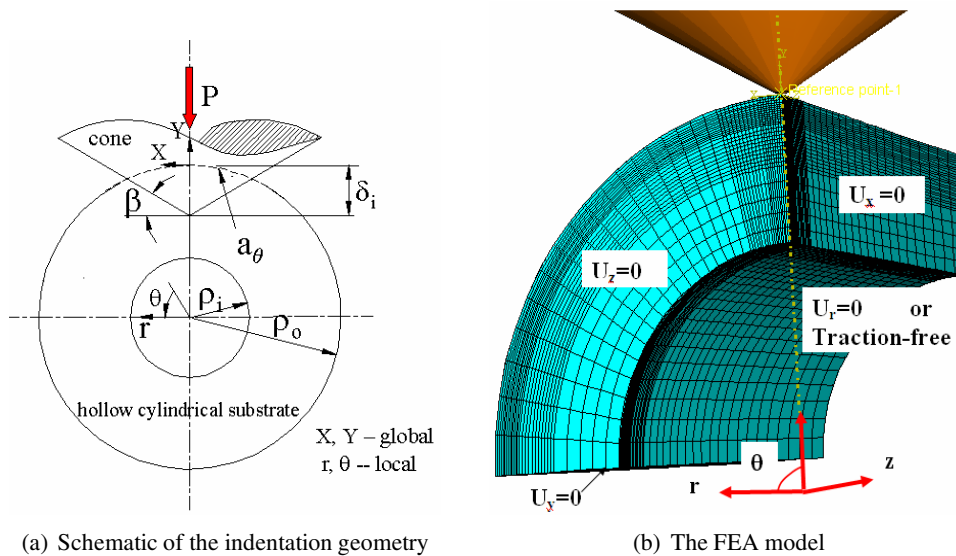


Figure 2: Indentation on a 3-D hollow cylindrical substrate

A typical finite element contact model is shown in Figure 2(b). 3-D isoparametric 8-node linear brick elements with incomplete modes, C3-D8I, have been chosen for the analysis. The inner surface is considered either to be traction-free or constrained such that $U_r=0$. A typical mesh consists approximately 43,000 user-defined elements and 700,000 total degrees of freedom plus the Lagrange Multiplier variables. A modified Ramberg-Osgood relationship is used to describe the uniaxial behavior of the substrate materials [6].

Conical indentation of a single-material cylindrical substrate can be examined using dimensional analysis. For conical indentation of a long solid cylindrical substrate, the compressive as well as the tensile biaxial strains on the contact surface in both the axial direction and the circumferential direction must be functions (f_a and f_c), of all the independent governing parameters. These include the Young's modulus (E), Poisson's ratio (ν), yield stress σ_Y , the inclination of the cone face to the surface of the cylinder in the axial direction β , the distance away from the

contact center, R_Z , R_θ , and the contact size, a_z a_θ :

$$\varepsilon_a^I = f_a(E, \sigma_Y, \nu, R_Z, a_z, \rho_0, \beta, \alpha, N) \quad (1)$$

$$\varepsilon_c^I = f_c(E, \sigma_Y, \nu, R_\theta, a_\theta, \rho_0, \beta, \alpha, N) \quad (2)$$

Using dimensional analysis [9], the following dimensionless functions, f_a and f_c , can be obtained:

$$\varepsilon_a^I = f_a \left(\frac{\sigma_Y}{E}, \frac{a_z}{\rho_0}, \frac{R_z}{a_z}, \beta, \nu, \alpha, N \right) \quad (3)$$

$$\varepsilon_c^I = f_c \left(\frac{\sigma_Y}{E}, \frac{a_\theta}{\rho_0}, \frac{R_\theta}{a_\theta}, \beta, \nu, \alpha, N \right) \quad (4)$$

Equation (3) expresses the indentation- induced biaxial in-plane strain state at each point on the cylindrical surface in the axial direction. The biaxial in-plane strain in the axial direction includes ε_{zz}^I and $\varepsilon_{\theta\theta}^I$ in the local r- θ -z coordinates. Equation (4) expresses the indentation-induced biaxial in-plane strain state at each point on the cylindrical surface in the circumferential direction. The biaxial in-plane strain in the circumferential direction also includes ε_{zz}^I and $\varepsilon_{\theta\theta}^I$ in the local r- θ -z coordinates.

From the dimensional analysis, it can be seen that the surface biaxial strains in the axial direction are dependent on a_z/ρ_w and R_z/a_z , and the surface biaxial strains in the circumferential direction are dependent on a_θ/ρ_w and R_θ/a_θ , for cases with otherwise identical contact conditions and material properties. Therefore, validation of the finite element models can be obtained by recognizing that the compressive, or tensile strain in a certain direction must be the same at the same R/a on different sizes of cylinders, but with the same a/ρ_w [6].

Results and Discussion

The results presented in Figure 3 are based on strain values from the 3-D numerical simulations. The relevant 2-D results presented for comparison are from 2-D simulations with the same material properties considered in the 3-D cases and with the same bond coat thickness of 110 μm . It is apparent that the stress intensity factors in the axial direction are very close to those from the 2-D analysis. This indicates that curvature effects on the stress intensity factors in the axial direction are negligible for the applied load levels used in the models. At the same time, the stress intensity factors in the circumferential direction are much larger at the same normalized distance away from the indent region.

It can also be seen that the stress intensity factor distributions at different load levels in the axial direction exhibit approximately the same characteristics as those of the 2-D flat specimen results. However, the stress intensity distributions for different load levels bear more evidence of load dependence in the circumferential

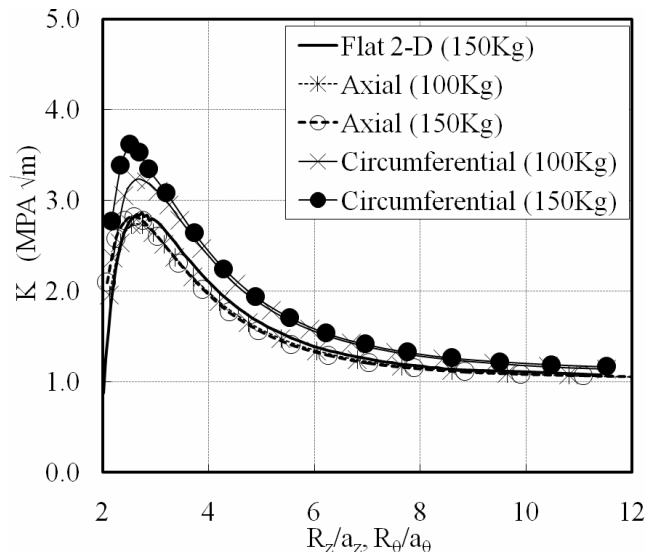


Figure 3: K vs. R/a for standard conical indenter contact on a hollow cylinder ($\rho_0 = 5.11$ mm, $\rho_i = 3.00$ mm) in the as-processed condition, with radial constraint on the inner surface.

direction. That is to say, curvature effects do not significantly influence the axial stress intensity factor distributions, but they do affect the circumferential stress intensity distributions. Similar phenomena are seen in the results for a small radius cylinder ($\rho_0 = 5.11$ mm, $\rho_i = 3.00$ mm) with constraints at the inner surface. When the inner surface is under traction free conditions, the results are similar to those with radial constraint. However, the analysis becomes more complex due to the effects of bending [6].

Concluding Remarks

The most important conclusion to be drawn from this work is that toughness measurement by indentation tests on cylindrical specimens may be approached via a 2-D analysis. However, results from a 3-D analysis are important for determining a valid test. Our detailed work [6] shows that stress intensity factors in the circumferential direction determine the debond size in that direction, which correspondingly determines whether or not buckling-driven delamination will occur. Thus, 3-D simulation results in the circumferential direction are very useful for preventing undesirable buckle-driven delamination and achieving a valid indentation test. At the same time, our detailed analyses reveal that the contact radii in the circumferential direction and the axial direction are not much different within the load levels of interest. Analyses further show that applied loads are very close to those from the 2-D models at the same penetration depth. Indentation simulations of practical cases reveal a very important characteristic – the results in the axial

direction are close to those of the model 2-D results. Results in the circumferential direction are not comparable to the 2-D results, exhibiting significantly larger stress intensity factor values.

References

1. Vasinonta, A.; Beuth, J.L. (2001). Measurement of interfacial toughness in thermal barrier coating systems by indentation. *Eng. Fracture Mech.*, 68, 843-860.
2. Handoko, R.A.; Beuth, J.L.; Meier, G.H.; Pettit, F.S.; Stiger, M.J. (2001). Mechanisms for interfacial toughness loss in thermal barrier coating systems. *Key Engineering Materials*, 197, 165-184.
3. Ma, Q.; Beuth, J.L.; Pettit, F.; Meier, G.H.; Stiger, M.J. (2005) Use of indentation fracture tests to investigate toughness loss mechanisms in thermal barrier coating systems. *Coatings 2005 Proc. Materials Science and Technology 2005*, Pittsburgh, September 2005, 3-6.
4. Ma, Q.; Beuth, J.L.; Meier, G.H.; Pettit, F.S. (2006) Indentation of a multi-layered solid cylinder for the measurement of thermal barrier coating adhesion. *Surface Protection for Enhanced Materials Performances Proc. Materials Science and Technology 2006*, Cincinnati, October 2006, 535-545.
5. Stiger, M.J.; Meier, G.H.; Pettit, F.S.; Ma, Q.; Beuth, J.L.; Lance, M. (2006) Accelerated cyclic oxidation testing protocols for thermal barrier coatings and alumina-forming alloys and coatings," *Materials and Corrosion*, 57(1), 73-85.
6. Ma, Q. (May, 2004). Indentation methods for adhesion measurement in thermal barrier coating systems. *Ph.D. Dissertation*. Carnegie Mellon University.
7. Bartsch, M.; Baufeld, B.; Fuller, Jr. E.R. (2003). Elucidating thermo-mechanical spallation of thermal barrier coating-systems using controlled indentation flaws *Ceramic Engineering and Science Proceedings*, 24(3), 497-502.
8. Mumm, D.R.; Watanabe, M.; Evans, A.G.; Pfaendtner, J.A. (2004). The influence of test method on failure mechanisms and durability of a thermal barrier system. *Acta Materialia*, 52(5), 1123-1131.
9. Barenblatt, G.I. (1996). Scaling, self-similarity, and intermediate asymptotics. *New York: Cambridge University Press*.